Metallophysics and Advanced Technologies
Металофіз. новітні технол.
Metallofiz. Noveishie Tekhnol.
2022, vol. 44, No. 5, pp. 659–669
https://doi.org/10.15407/mfint.44.05.0659
Reprints available directly from the publisher

PHYSICS OF STRENGTH AND PLASTICITY

PACS numbers: 61.72.U−, 81.05.-t, 81.05.Bx, 81.10.-h, 81.20.-n

Influence of Fly Ash on Microstructure and Mechanical Properties of Aluminium (Al/7Si) Alloy Composite

Chirav Shah, Denish Raiyani, Hem Dave, K. Santhy,
and J. Muthukumar*

Indus University, Institute of Technology and Engineering,
Department of Materials and Metallurgical Engineering,
Rancharda, Ahmedabad-382115, India
**CARE Group of Institutions,*
Department of Mechanical Engineering,
27 Thayanur, Tiruchirappalli-620009, Tamil Nadu, India

Metal matrix composites (MMC) have a wide range of applications in today's world, due to their high strength to weight ratio. In the present work, aluminium alloy LM25 and fly ash are selected as matrix and reinforced materials, respectively. Fly ash is a waste product in thermal power plants. Its ease availability in low cost can be converted into useful product. MMC of aluminium alloy LM25—with 5 and 7.5% wt. fly ash composite is made by stir casting. The composite mechanical properties are compared with aluminium alloy. The chemical composition of aluminium alloy and its composite are studied by optical emission spectroscopy. The mechanical properties such as tensile strength, elongation and hardness are obtained by employing UTM and Brinell hardness tester. The specimens' microstructure and phase analysis are studied using an optical microscope and XRD. A segregation of fly ash is found in the grain boundaries in the microstructure. The mechanical properties show significant enhancement from the base metal. The various defects present in the casting are studied with the help of radiography technique.

Key words: fly ash composite, stir casting, mechanical properties, microstructure analysis, radiographic testing.

Металоматричні композити завдяки високому значенню відношення мі-

Corresponding author: Kathirvel Santhy
E-mail: k_santhy@rediffmail.com

Citation: Chirav Shah, Denish Raiyani, Hem Dave, K. Santhy, and J. Muthukumar, Influence of Fly Ash on Microstructure and Mechanical Properties of Aluminium (Al/7Si) Alloy Composite, *Metallofiz. Noveishie Tekhnol.*, **44**, No. 5: 659–669 (2022).
DOI: 10.15407/mfint.44.05.0659

цности до ваги мають широкий спектр застосувань в сучасному світі. У даній роботі в якості матричного і посилювального матеріялів обрано алюмінійовий стоп LM25 і золу виносу. Зола виносу є відходом теплових електростанцій. Її легка доступність та низька вартість дозволяє перетворити її у корисний продукт. Металоматричні композити алюмінійового стопу LM25 із 5 і 7,5% мас. золи виносу виготовлялися методою лиття із перемішуванням. Механічні властивості композиту близькі до властивостей алюмінійового стопу. Хемічний склад алюмінійового стопу та композиту досліджено методами оптико-емісійної спектроскопії. Механічні властивості, а саме міцність на розрив, подовження та твердість, визначено методою Брінелля. Дослідження мікроструктури та фазова аналіза зразків проведено за допомогою оптичного мікроскопа та рентґенівської аналізи. Виявлено сеґреґацію золи виносу у межах зерен. Механічні властивості суттєво поліпшуються у порівнянні з базовим металом. Дефекти, наявні у виливку, вивчено за допомогою рентґенографії.

Ключові слова: зольний композит, лиття з перемішуванням, механічні властивості, мікроструктурна аналіза, рентгеноґрафічні дослідження.

(Received December 31, 2020; in final version, January 4, 2022)

1. INTRODUCTION

Macroscopic combination of two or more materials is called as composite. One of the major materials being metal and the other one, usually a non-metal, is called metal matrix composite (MMC). In the past few years, MMCs have gained more famous because of their low density, high strength, high stiffness, damping capacity, good wear resistance, better fatigue resistance and lower creep rate compared to conventional alloys [1, 2]. Aluminium matrix ceramic reinforcement composites have attracted increasing attention due to their combined properties such as high specific strength, high stiffness, low thermal expansion coefficient and superior dimensional stability at elevated temperatures as compared to the monolithic materials. This has led to it being an important material for the automotive and aerospace industries [3–5]. There are many ways to fabricate metal composite including powder metallurgy, pressure infiltration, casting, diffusion bonding and spray co-deposition. After considering cost and ease of fabrication, stir casting method was chosen. Stir casting is a process in which dispersed phases like ceramics are incorporated in the molten metal matrix of metal (Fig. 1). They are then mechanically stirred, followed by solidification. The stirring action leads to improvement in the distribution of fly ash and its wettability. Content of dispersed phase in MMC via stir casting is limited to 30% [6]. The distribution of the dispersed phase in the matrix must be homogeneous. There might be segregation because of the difference in density which might lead to the formation of clusters.

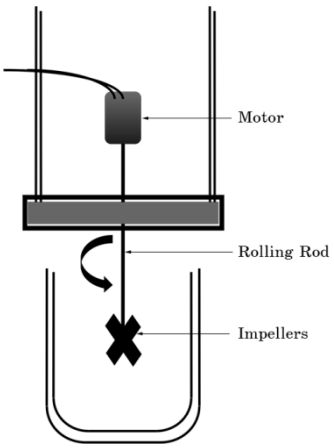

Fig. 1. Schematic diagram of the stirrer.

Fly ash is a by-product of thermal power plants which is not used conventionally and thought of as a waste by-product. It is used as a reinforcement material in this study. In India, 110 million tons of fly ash is generated every year [7]. In general, fly ash consists of silicon oxide, alumina, and iron oxide as major constituents and oxides of Mg, Ca, Na, K, *etc.* as minor constituents. Fly ash particles are mostly spherical in shape and range from less than 1 to 100 μm. Due to fly ash being a waste by-product, they are available for very low cost. In addition, fly ash is a non-shrink material. They have great workability, high stiffness and low thermal expansion coefficient.

Aluminium matrix is strengthened by the addition of hard and brittle fly ash particles. Due to fly ash being low cost and abundantly available, it helps in overcoming the cost barrier in the widespread application of aluminium in automotive and small engine applications. Additionally, greenhouse gases are minimized using fly ash which substitutes aluminium in the production of aluminium alloys. Aluminium alloy fly ash composites are a potential material for highway and runway signs, sliding tracks for windows and doors, automotive parts, industrial furniture, machine cover, frames and ducts and similar places [8].

TABLE 1. Chemical composition of fly ash [18].

Oxides	SiO_2	Al_2O_3	Fe_2O_3	CaO	MgO	TiO_2	Na_2O	K_2O	SO_3	Loss of ignition
% wt.	57.1	27.1	7.4	2.1	1.2	1.2	0.22	2.2	0.1	1.3

The fly ash reinforced composite has been studied for different systems, such as Al–fly ash [6, 9–11], Al–4.5% Cu–fly ash [1], AA6063–fly ash [2], AA6061–fly ash [12], A535–fly ash [13], Al6061–fly ash [14], AA6061–Al_2O_3–fly ash [15], Al–3Cu–8.5Si–fly ash [16], Al–12Si–fly ash [10] and A535–SiC–fly ash [13]. With an increase in fly ash hardness, tensile and compressive strength of MMC is improved [1, 7, 17]. However, these mechanical properties decrease when fly ash becomes more than 20% wt. [7]. The commercial LM25 alloy of aluminium is used in chemical and automobile industries. The effect of fly ash in LM25 is not studied much. Present work concentrates on the influence of fly ash in LM25 Al alloy. In addition, the sound casting was inspected through radiographic testing.

2. EXPERIMENTAL DETAILS

Aluminium LM25 alloy was melted in graphite crucible. In induction furnace, 16 kW of power was supplied to melt LM25. After LM25 was melted completely and converted to a liquid state, fly ash was added with 3 different compositions such as 0, 5 and 7.5% wt. More content of fly ash was not chosen in order to maintain the corrosion resistance [10] of the composite. A three-bladed impeller made of mild steel driven by an electrical motor acts as a stirrer which is dipped into the melt. During the stirring process, the fly ash was added in batches to ensure homogeneous mixing. The schematic diagram of a mechanical impeller dipped in molten metal is shown in Fig. 2. After enough mixing, the melt was poured into the cleaned cylindrical-shaped mild steel die. Its chemical composition is mentioned in Table 1. In Optical Emission Spectrometer (OES), the specimen is vaporized with the testing probe by a spark of an arc discharge to determine its composition. Shimadzu OES-5500 spectrometer was used to find out the composition of LM25 alloy and its composites. An optical microscope was used to study the

TABLE 2. Chemical analysis of commercial and fly ash reinforced LM25 Al alloy (in % wt.).

Fly ash	Cu	Mg	Si	Fe	Mn	Ni	Zn	Pb	Ti	Sn	Al
0	0.14	0.60	7.33	0.50	0.15	0.03	0.08	0.05	0.02	0.02	90.18
5	0.14	0.58	8.12	0.62	0.15	0.04	0.09	0.05	0.08	0.04	90.20
7.5	0.15	0.32	8.30	1.00	0.17	0.09	0.09	0.04	0.02	0.01	89.58

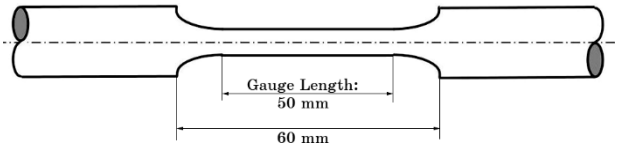

Fig. 2. Tensile specimen's dimensions.

microstructure of the base metal and its composite materials. Hydrofluoric acid was used as etchant with 0.5% concentration. The microstructures of all these samples were taken at 200X magnifications.

As shown in Figure 2, the ensile specimen was prepared with 50 mm gauge length and 11.28 mm diameter. The tensile test was conducted using a computerized tensile testing machine. Hardness measurements were carried out on the base metal and composite samples by using a Brinell Hardness Machine with ball indenter. The average value of three measurements was reported. Radiography test (Dandong Zhong Yi NDT Co., Ltd., China) was performed to detect and determine the distribution of pores inside the tensile sample.

Tescan SBH VEGA3 model SEM was employed to measure the particle size of fly ash. Presence of various phases of fly ash, LM25 alloy and fly ash reinforced Al alloy composite was identified with the help of XRD (MiniFlex Rigaku, Japan).

3. RESULTS AND DISCUSSION

The chemical composition of LM25 and fly ash reinforced LM25 composite determined by OES is shown in Table 2. The Si and Fe content increases with the addition of fly ash content. That implies, fly ash was getting indeed incorporated in the matrix.

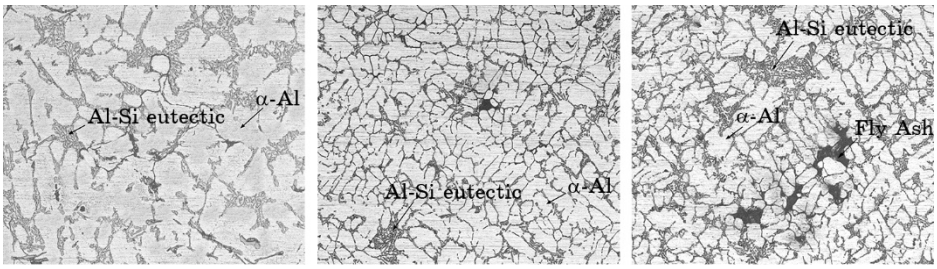

Fig. 3. Optical microstructures of LM25 Al alloy (*a*), 5% fly ash reinforced LM25 Al Alloy composite (*b*), 7.5 wt.% fly ash reinforced LM25 Al alloy composite using HF as the etchant (*c*).

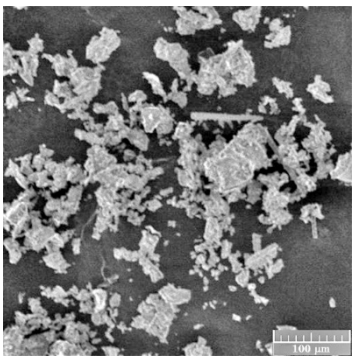

Fig. 4. SEM image of fly ash.

Figure 3 shows the microstructure of commercial LM25 Al alloy and fly ash reinforced composites using hydrofluoric acid as an etchant. The microstructure reveals the presence of α-Al and Al–Si eutectic phases as per hypoeutectic Al–Si system. In addition to porosity, non-uniform distribution of fly ash is observed in MMC. The agglomerated fly ash particles are seen at the grain boundaries of 5–7.5% wt. fly ash reinforced composites. Gikunoo *et al.* [13] reported a similar finding that non-uniform distribution of fly ash likes to segregate in grain boundaries and promotes porosity. Rajan *et al.* [19] mentioned that for uniform distribution fly ash, it must be surface treated in acid solution by employing ultrasonic vibration and heat-treated before adding in liquid metal.

As per intercept method, the grain sizes of the microstructure (Fig. 3) are 6.7, 8.4, and 8.6 for LM 25 alloy, 5 and 7.5% wt. reinforced fly ash composite, respectively. The fly ash acts as a grain refiner and does

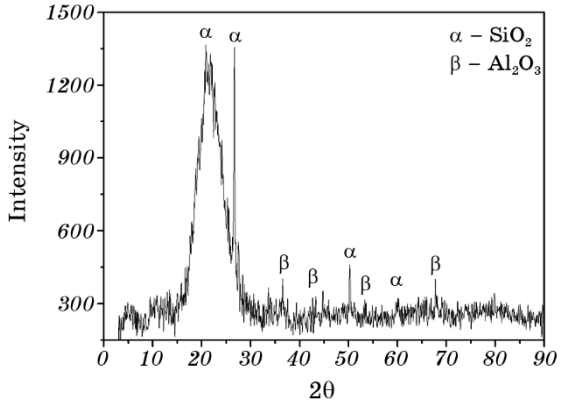

Fig. 5. XRD pattern of fly ash.

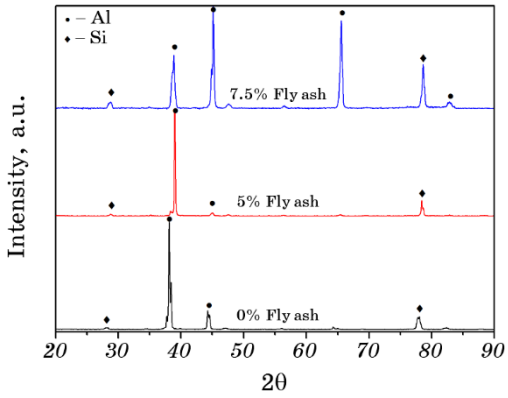

Fig. 6. XRD pattern of 0, 5 and 7.5% wt. of fly ash reinforced LM25 Al alloy.

not show much difference in grain size between 5 and 7.5% wt. fly ash reinforced composite. This might be one of the reasons for better mechanical properties.

Figure 4 shows the SEM image of fly ash particles. It indicates that fly ash has a wide range size distribution (6–80 μm) in irregular shapes and agglomeration. These agglomerates promote porosity in MMC.

The XRD pattern of as-received fly ash and cast fly ash reinforced LM25 Al alloy are shown in Figs. 5 and 6, respectively. The major content of fly ash is SiO_2 and Al_2O_3 which is revealed in the XRD pattern. Presence of Fe_2O_3 peaks suppressed with low phase fraction and noises due to impurities. As mentioned by Al–Fe–Mg–Si phase diagram [19], $Al + Si + Al_5FeSi + Al_5FeMg_3Si_8$ phases are expected in the XRD pattern of LM25 alloy and MMC. Due to low phase fraction, ternary and qua-

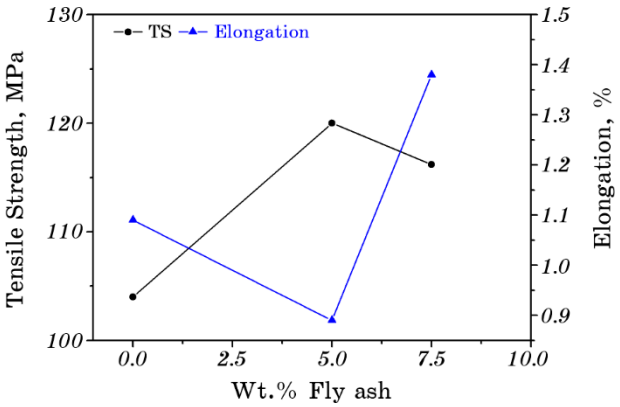

Fig. 7. Tensile strength and elongation with respect to fly ash content in LM25 alloy.

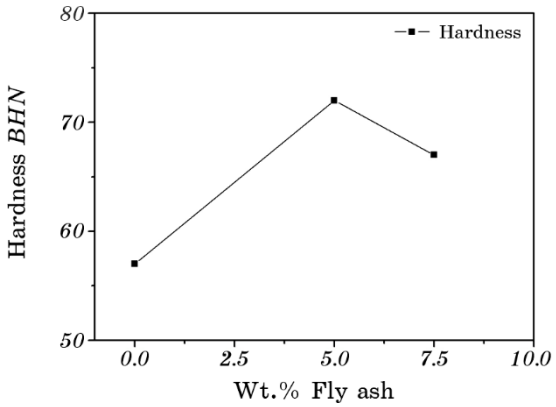

Fig. 8. Hardness of the specimens with respect to the increase in the fly ash content.

ternary intermediate phases are not observed in XRD and also in the microstructure. Figure 6 shows that the intensity of Si peak is increased with the addition of the fly ash content in Al alloy. It may be due to the interfacial reaction between fly ash and aluminium matrix as mentioned by Rajan *et al.* [20] and Zahi and Daud [21]. Hence, the probability for the formation of iron intermetallic is very low in MMC. As mentioned by Rajan *et al.* [20], the possible interfacial reactions of fly ash with the matrix are

$$2Al_{(l)} + Mg_{(l)} + 2SiO_{2\,(s)} \rightarrow MgAl_2O_{4\,(s)} + 2Si_{(s)}, \quad (1)$$

$$3Mg_{(l)} + 4Al_2O_{3\,(s)} \rightarrow 3MgAl_2O_{4\,(s)} + 2Al_{(l)}. \quad (2)$$

The XRD pattern did not reveal the presence of $MgAl_2O_4$ due to poor quantity. Tensile strength and elongation trend of specimens are shown in Fig. 7. The tensile strength of MMC is higher than LM25 al-

Fig. 9. Tensile specimens after testing.

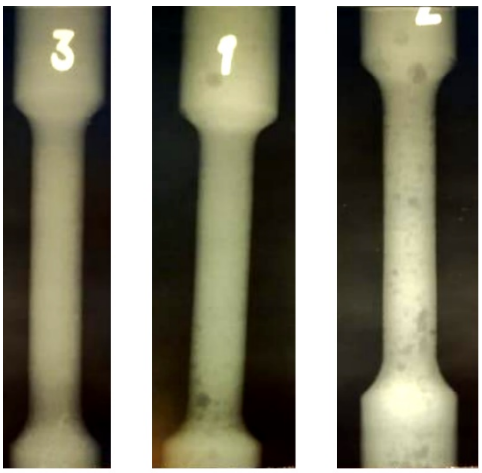

a *b* *c*

Fig. 10. Radiography image of LM25 Al alloy (*a*), 5% wt. fly ash reinforced MMC (*b*), 7.5% wt. fly ash reinforced MMC (*c*).

loy and it also increases with fly ash content. The tensile strength decreases after 5% wt. because of loss in interfacial bonding between the reinforced particles (fly ash) and matrix phase (LM25). It should be noted that the tensile strength is still higher in 7.5% wt. than in pure LM25. It is mainly due to the interaction of dislocations and fly ash. It can be inferred from the graph that the above phenomenon occurs because of the agglomeration of particles in the grain boundary.

In addition, the strength of fly ash reinforced composite is increased due to reduction in grain size as per the Hall–Petch equation [22]

$$\sigma = \sigma_0 + Kd^{-1/2}, \tag{3}$$

where σ is the strength of the alloy, σ_0 is a material constant which gives resistance to dislocation movement, K is strengthening coefficient and d is grain size. The broken-up tensile pieces are shown in Fig. 9. The controversial tensile test result of 7.5% wt. fly ash composite further analysed using radiography test.

Hardness of each phase is different. Figure 8 shows the hardness of base materials and its composites. The trend of the hardness is very similar to tensile strength of the specimens. It shows that the addition of fly ash increases the hardness when compared to Al alloy. The decrease in hardness and tensile strength of 7.5% wt. fly ash reinforced composite must be cross verified with defects.

Figure 10, *a* shows the LM25 alloy (0% wt. fly ash) radiography image which is free from defects. Figure 10, *b*, *c* shows radiography images of 5 and 7.5% wt. fly ash reinforced Al alloy composites, respec-

tively. The spherical and irregular sports are observed throughout the sample. A dark spherical sport indicates the presence of gas porosity. Normally, the gas porosity in casting is formed due to insufficient size of sprue or and poor mould preparation, *i.e.*, too fine, too wet or low permeability sand usage. However, LM25 alloy, *i.e.*, absence of fly ash does not have gas porosity which is clearly seen in Fig. 10, *a*. It indicates that fly ash introduces the gas porosity in the composite. An irregular dark spot in radiography images indicates the agglomeration of fly ash, which is not observed uniformly. It is mainly due to untreated fly ash and low RPM of stirrers. In the x-ray radiography images, it can be seen that the irregularly shaped black spots multiply with an increase in fly ash content. This leads to a conclusion that porosity distribution and an agglomerated fly ash particle reduces the mechanical properties such as tensile and hardness of 7.5% wt. fly ash reinforced MMC.

4. CONCLUSIONS

Fly ash can turn industrial waste into industrial wealth. Its usage in the composite can solve the problem of storing and disposal of fly ash. Influence of fly ash in LM25 was studied in terms of its mechanical and metallurgical analysis in addition to radiography testing. Increase in fly ash content in LM25 alloy increases in tensile strength and hardness compared to the base metal. The untreated fly ash in MMC agglomerates and adversely promotes porosity. Present work indicates that

– surface treatment of fly ash is necessary to avoid agglomeration in MMC,

– sound casting must be verified by NDT Co. before optimizing fly ash content *vs.* properties,

– the mechanical properties of LM25 Al alloy improved by addition of fly ash.

REFERENCES

1. K. Mahendra and K. Radhakrishna, *Mater. Sci. Pol.*, **25**: 57 (2007).
2. A. Mohammed Razzaq, D. L. Majid, M. R. Ishak, and U. M. Basheer, *Metals*, **7**: 477 (2017).
3. D. J. Lloyd, *Int. Mater. Rev.*, **39**: 1 (1994).
4. M. Fujine, T. Kaneko, and J. Okijima, *Adv. Mate. Process.*, **143**, No. 6: 20 (1993).
5. J. Goni, I. Mitxelena, and J. Coleto, *Mater. Sci. Techno.*, **16**: 743 (2000).
6. D. Mohana Rao and M. E. Bapi Raju Bandam, *IJISME*, **13**, No. 1: 1 (2014).
7. P. Shanmughasundaram, S. Ramanathan, and G. Prabhu, *Eur. J. Sci. Res.*, **63**, No. 2: 204 (2011).

8. P. K. Rohatgi, R. K. Guo, H. Iksan, E. J. Borchelt, and R. Asthana, *Mater. Sci. Eng. A*, **244**, No. 1: 22 (1998).
9. S. Sarkar, S. Sen, S. Mishra, M. K. Kudelwar, and S. Mohan, *J. Reinf. Plast. Compos.*, **29**: 144 (2010).
10. K. Radhakrishna and M. Ramachandra, *Wear*, **262**: 1450 (2007).
11. M. Raja Kumar, M. Shunmuga Priyana, and A. Mani, *IJSER*, **5**, No. 5: 1261 (2014).
12. J. David Raja Selvam, D. S. Robinson Smart, and I. Dinaharan, *Mater. Des.*, **49**: 28 (2013).
13. E. Gikunoo, O. Omotoso, and I. Oguocha, *Mater. Sci. Technol.*, **21**: 143 (2005).
14. H. C. Anilkumar, H. S. Hebbar, and K. S. Ravishankar, *IJMME*, **6**, No. 1: 41 (2011).
15. Yashpal, Narender Panwar, M. M. Goud, and Suman Kant, *Mater. Today: Proc.*, **5**, No. 14: 28413 (2018).
16. Krishnan Ravi Kumar, Kothavady Mylsamy Mohanasundaram, and Ramanathan Subramanian, *De Gruyter*, **21**, No. 2: 181 (2014).
17. S. M. Russel Kabir Roomey, *AJER*, **6**, No. 12: 334 (2017).
18. Deepa A Sinha, *Int. J. Emerging Technol. Adv. Eng.*, **4**: 5 (2014).
19. Vadim S. Zolotorevsky, Nikolai A. Belov, and Michael V. Glazoff, *Casting of Aluminum Alloys* (Amsterdam: Elsevier: 2007), p. 327.
20. T. P. D. Rajan, R. M. Pillai, B. C. Pai, K. G. Satyanarayana, and P. K. Rohatgi, *Compos. Sci. Technol.*, **67**: 3369 (2007).
21. S. Zahi and A. R. Daud, *Mater. Des.*, **32**, Iss. 3: 1337 (2011).
22. E. O. Hall, *Proc. Phys. Soc. B*, **64**: 747 (1951).